ELSEVIER

Coordination Chemistry Reviews 233–234 (2002) 255–271

COORDINATION CHEMISTRY REVIEWS

www.elsevier.com/locate/ccr

Synthesis, characterization and reactivity of some macrobicyclic and macrotricyclic hetero-clathrochelate complexes

Alison Ingham [a], Mary Rodopoulos [b], Kevin Coulter [c], Theo Rodopoulos [d], S. Subramanian [e], Alex McAuley [f,*]

[a] *Health Canada, Ottawa, Ont., Canada*
[b] *Institute of Drug Technology, Vic., Australia*
[c] *Department of Chemistry, Memorial University, St. John's Newfoundland, Canada*
[d] *CSIRO, Clayton, Vic., Australia*
[e] *Department of Chemistry, University of BC, Vancouver, BC, Canada*
[f] *Department of Chemistry, University of Victoria, Elliot Building, P.O. BOX 3055, Victoria, BC, Canada V8W 3V6*

Received 16 October 2001; accepted 15 February 2002

This article is dedicated to colleague and good friend Barry Lever in honor of his 65th birthday

Contents

Abstract

A variety of synthetic procedures, including organic reagents and templated metal ion reactions have led to new and interesting ligand sources. This review focuses principally on the preparation of macrobicyclic and macrotricyclic systems based upon a cyclam framework into which a wide range of cations can be incorporated. Emphasis is placed on ligand synthesis and characterization, particularly by X-ray crystallography, to confirm the location and coordination geometry of the encapsulated ions. The range of ligands described includes proton sponges, and frameworks containing different types of coordinating donors. Emphasis is placed on the formation of a tetraaza-(cyclam) base onto which are attached either one or two pendant rings. The resulting metal complexes show enhanced thermodynamic stability and kinetic inertness. Metal ions from various parts of the Periodic Table are used as examples of the ability of these ligands to form complexed ions and to accommodate differing coordination preferences of the ions.

* Corresponding author. Tel.: +1-507217164; fax: +1-2507217147.
E-mail address: amcauley@uvic.ca (A. McAuley).

PII: S0010-8545(02)00031-0

A short section is included on the redox properties of some transition metal ions, principally nickel and copper where stabilization of a higher oxidation state in the former leads to new chemistry not generally seen in mono-macrocyclic complexes.

Keywords: Macrobicyclic; Hetero-clathrochelate; Reactivity

1. Introduction

For nearly 40 years, since the pioneering work of Curtis [1], Busch [2] and others, there has been an interest in the kinetic and thermodynamic stability of macrocyclic complexes. Much of the work has been reviewed [3–15], particularly as larger-sized rings with an increased number and variety of donors, and new complexes have been developed in many areas.

A recent theme in the synthesis of macrocyclic metal ions has been the extension of the ligand framework by use of pendant, or, additional smaller macrocyclic arms, capable of both inter- and intra-molecular coordination. Such species result in both mono- and polynuclear complexes with constrained donor environments, but with the potential for specific site substitution [16–18]. A second area of interest is the coordination of metal ions by macrotricyclic ligands, wherein the possibility exists of complete encapsulation of the metal center, resulting in complexes that are incapable of undergoing simple substitution reactions [19] that may be exemplified by the azacryptates of Sargeson. The preparation and reactivity of the latter have been described [20,21] together with some recent novel systems with appended additional groups making the complexes useful as potential radio-imaging materials. These studies have been well documented and will not be commented on further in this article.

Many of the polycyclic amines described impart thermodynamic stability and kinetic inertness to a variety of oxidation states. This is particularly true of Ni(I), Ni(II) and Ni(III) complexes that have been the subject of study [21–27]. Several of the ligands synthesized include a pendant arm donor attached to the cyclam (1,4,8,11-tetraazacyclotetradecane) unit. Although such species impose pseudo-octahedral or five-coordinate geometries at the metal center, they generally exhibit acid lability owing to facile protonation of the pendant arm unit [28]. This deficiency has been overcome by integrating the pendant arm as a small macrocycle into the cyclam framework in a macrobicyclic manner, providing not only greater acid protection, but also increased thermodynamic stability.

This review will focus predominantly on the synthesis of macrobicyclic and macrotricyclic ligands, and the spectroscopic, redox and kinetic aspects of the complex ions formed. In the case of the macrobicyclic systems, no mention will be made of bridged cyclic units that have been the subject of a recent review [15].

2. Tetraaza-based macrobicycles

2.1. Ligand synthesis

Two major methods have been used in the preparation of polymacrocyclic ligands.

2.1.1. Organic reactions

The first, based on conventional organic synthesis, relates to previous studies that used either the Richman Atkins [29] approach, and later, a claw-like precursor developed by Bradshaw et al. [30]. Other approaches have reacted cyclam [31] and 1,4,7,10-tetraazacyclododecane (cyclen) [32–35] with organic bridging units.

Structurally, the simplest tetraazamacrobicycle is one where the cyclic tetraamines are strapped by an alkylene chain across two non-adjacent nitrogen atoms (Scheme 1). Springborg et al. [34,36] has pioneered some elegant work in the preparation of bowl-shaped adamanzanes (e.g. 12,17-dimethyltetraazaaabicyclo[7.5.5]nonadecane) and their metal complexes. As an example, the bicyclic tetraamine 1,4,7,10-tetraazabicyclo[5.5.3]pentadecane, (**1**), has been synthesised [35] by reaction of the 1,7-bis-ditosylate of cyclen with the ditosylate of propane diol, followed by the removal of the tosyl groups [29]. The corresponding system with a tetramethylene bridge, **3,** has been prepared [31] by reaction of the di-acid chloride with the di-protected tetraazamacrocycle. The intermediate diamide, **2**, was reduced by use of diborane in thf to yield **3**, a potent proton sponge.

The di-aza-protected ligand, Me_2 cyclen, has also been used as a starting material for the formation of the

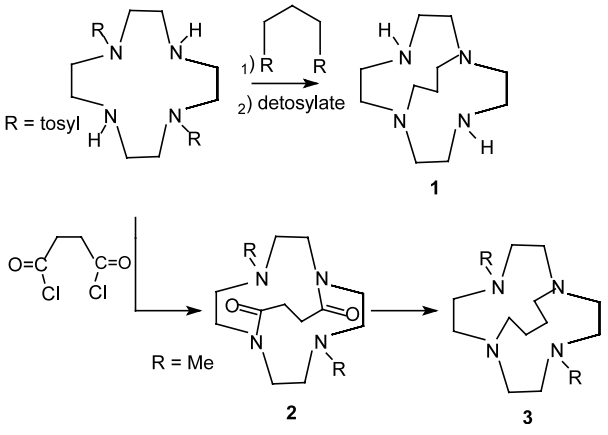

Scheme 1. Synthesis of ligands **1** and **3**.

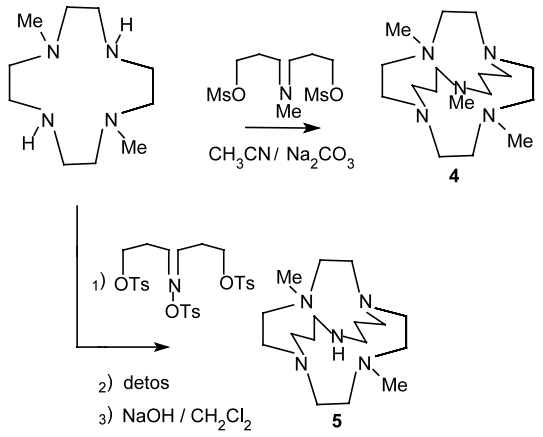

Scheme 2. Synthesis of ligands **4** and **5**.

aza cage, **4,** [37] (Scheme 2). In this reaction, a potentially penta-coordinate ligand system is formed, although the cyclen ring is too small to incorporate transition metal ions. The corresponding ligand with a bridging NH moiety, **5**, has also been synthesized [33], as has the corresponding adamanzane (12,17-dimethyltetraazaaabicyclo[7.5.5]nonadecane) with a 4-azaheptalene bridge between the 1,12-nitrogen atoms of the cyclen [38]. The ligand **6**, where the protected groups are on adjacent nitrogen atoms, has been prepared together with the Mn(II) and Fe(II) complexes [39]. Reinforced cyclam systems such as **7**, have been shown to impinge on the spin states of some nickel complexes [40].

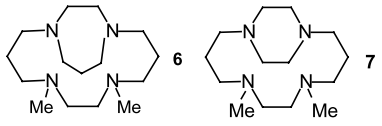

The synthesis [41] of the macrobicyclic ligand 14-oxa-1,4,8,11-tetraazabicyclo[9.5.3]nonadecane (**8**), that is capable of encapsulating transition metal ions, involved the reaction in acetonitrile (Scheme 3) of the ten-membered macrocycle 1-oxa-4,8-diazacyclodecane, [10]-aneN_2O, (**9**), (prepared via the Richman and Atkins tosylate method [29], with conc. H_2SO_4 as detosylating

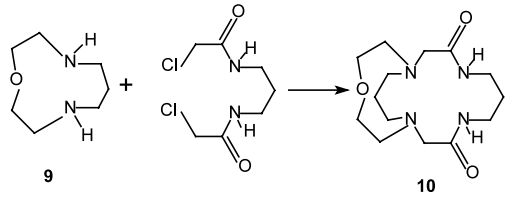

Scheme 3. Synthesis of ligand **10**.

agent) and 1,3-bis(α-chloroacetamido)propane (formed by use of an adaptation of the method described by Bradshaw [30]), leading to the diamide **10**.

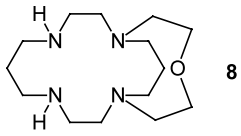

Reduction of **10** with BH_3–thf, yielded the macrobicycle **8** in good yield. Ligands **11** [42] and **12** [43] have been reported.

The isomers (**12**, **14**) of the N_4X series have the bridges between the 1,8-*trans*-nitrogens of cyclam. Complexes formed by this ligand have a 'hemicryptate' structure. This ligand has been prepared recently [31], using essentially the bridging synthetic route described herein, but the process required selective separation of **12** from the variety of organic products formed. A two-step process has also been reported by the authors where protection of aza-sites on the cyclam ring is afforded by use of the *trans*-dioxo-diamide [43]. These versatile syntheses have also been performed with cyclen as starting material. However, in the reactions with the dioxo-cyclen with a bis-electrophilic spacer, only macrotricycles are formed [44]. A different approach to separation of the ligand mixtures derived in the synthesis of **12** has been used recently [45] by complexation of the ligand mixture with Cu(II) and subsequent chromatographic separation as metal ion complexes. Each ligand can then be isolated by reaction with Na_2S with removal of the copper(II) ion.

Two interesting dipyridyl-containing macrobicycles have been described recently [46] for the formation of

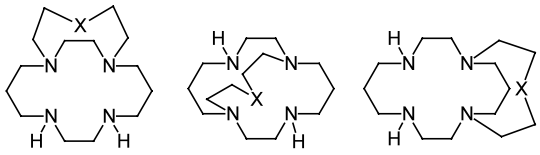

lanthanide complexes. Ligand **17** was prepared by reaction of **18** by reaction with 6,6′-bis(bromomethyl)-2,2′-dipyridyl in acetonitrile in the presence of base. The synthesis of systems incorporating both pyridine **19** and biisoquinoline (not shown) units has been described [47] and crystal structures of the lithium complexes determined [48]. A hexa-protonated cryptate macrobicyclic cation [49] has been shown to encapsulate perchlorate and nitrate ions.

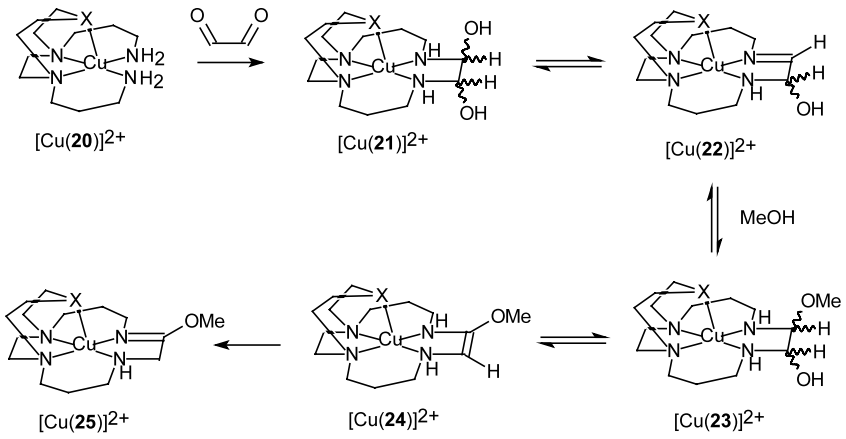

Scheme 4. Mechanistic interpretation of the synthesis of imidate complex $[Cu(\mathbf{25})]^{2+}$.

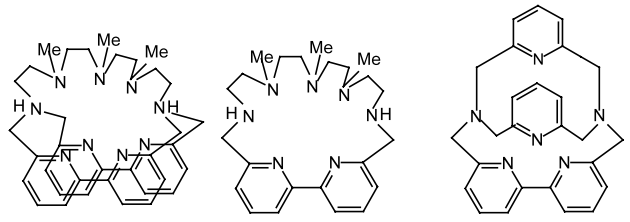

2.1.2. Template synthesis

The second approach that has been used involves the formation of a complexed metal ion as a template within which further reaction of the coordinated ligand may take place. Examples of this type have been seen in earlier investigations to produce macrocyclic ligands of varying size [1,3–5,13,23,49–51]. In this approach, there is generally a higher possibility of reaction to a specific target. Interestingly, the synthesis of a macrocycle has been described in which an internal hydrogen-bonding network acts as a template [52].

The involvement of metal ion templates has been extended to the formation of macrobicyclic species [41,53,54]. In Scheme 4 (X = O, S, NH) is presented the generalized mechanism for a glyoxal condensation [54], based on the nature of the intermediates isolated and on deuterium-exchange experiments. In the sequence shown, the formation of a variety of products, not normally isolated, has been identified. Templates, such as $[Cu(\mathbf{20})]^{2+}$, were derived from Michael addition adducts of 1,4,7-tri-aza-,1,4-di-aza-7-oxo-, and 1,4-diaza-7-thia-cyclononane with acrylonitrile, followed by reduction with BH_3–thf [42–54] to yield ligands **11**, **13**, and **16**, respectively. There is a contrast in the reactivities of copper(II) and nickel(II) templates in these condensations. In the mono-macrocycle (cyclam) formation, nickel(II) is the ion of choice [55], with very poor reactivity recorded for copper(II). However, in the formation of the macrobicyclic species under consideration, the reagent of choice is the Cu(II) ion, possibly owing to the formation of a five-coordinate intermediate. The latter ion may be readily removed from the complex by aqueous reaction with Na_2S, followed by extraction into an immiscible solvent (chloroform or dichloromethane).

The formation of the copper(II) complex increases the kinetic inertness and thermodynamic stability of relatively novel species. The majority of nickel(II) templated Schiff base condensations with glyoxal have been shown to yield the expected diimine intermediate which may then be reduced to the corresponding saturated macrocycle [49]. However, depending on the degree of dehydration that occurs during the Schiff-base condensation, there are three different possible products: the dicarbinolamine, **21** imine-carbinolamine **22** and a diimine. Ideally, the fully dehydrated diimine complex might be expected. In the bicyclic systems, steric forces associated with the coordinated ligand are too great to allow the formation of a planar, five-membered diimine ring around the metal center. The hydrated and semi-hydrated five-membered rings retain more flexibility with much less strain in the ring by averting the need for planarity.

3. Tetraaza-based macrotricyclic ligands

Routes taken in the synthesis of macrotricyclic ligands have generally involved organic precursors. For example, ligand **27** has been prepared [56] by the prior formation of 4,8-(dichloroacetyl)-1-oxa-4,8-diazadecane (Scheme 5) as an intermediate that was further reacted with the ten-membered macrocycle to give the diamide 7,16-dioxa-1,4,10,13-tetraazatricyclo[11.5.3.3]octadecane 3,11-dione, **26**. This ligand was reduced as described to yield the saturated tricyclic ligand **27**.

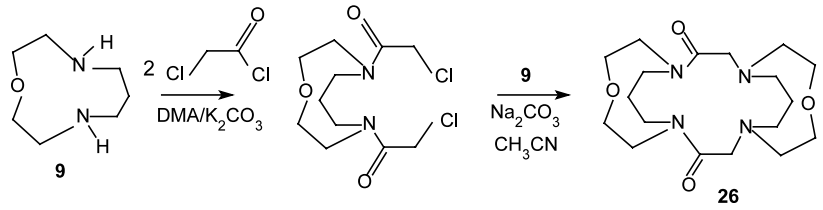

Scheme 5. Synthesis of ligand **26**.

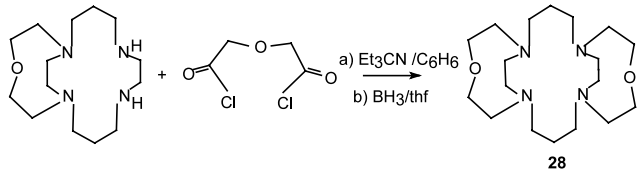

Scheme 6. Synthesis of ligand **28**.

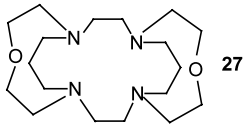

Dissolution of the free ligand in water, and addition of 0.1 M $HClO_4$ gave white crystals of the diprotonated species $[H_2(\mathbf{27})](ClO_4)_2$.

The isomeric tricycle, **28**, in which the pendant rings are 9-membered units, has been synthesised [56,57] as shown in Scheme 6. Unlike ligand **27**, this macrotricycle cannot adopt the *trans*-III conformation of cyclam [58].

The corresponding thioether systems have also been prepared [59]. In this instance, for the bis-9-membered ring system, reaction of cyclam with 4 moles of chloroacetyl chloride (Scheme 7) followed by ring closure with sodium sulfide, and subsequent reduction gave the macrotricycle **29** in good yield.

As in the case of the bis-ether analogue, the ligand can adopt both *syn*- and *anti*- configurations. The isomeric ligand, **30**, with larger ten-membered rings has also been prepared [59] by reaction of macrocycle **15** with $(BrCH_2CH_2)_2S$ as outlined in Scheme 8.

Macrotricyclic complexes containing two cyclam units have been prepared by use of the protected dioxocyclam **31** [60]. As shown in Scheme 9, reaction with Boc to protect one of the aza sites, followed by reaction with 0.5 equivalents of α,α′-dibromo-*m*-xylene led to the bridged bis macrocycle **32**. After removal of the Boc, further reaction with the xylene and reduction of the tricyclic tetraamide, the fully reduced macrotricycle **33** was isolated, in an overall yield of about 27%.

The synthesis of two new tricyclic complexes based on cyclam has been described [61]. Reaction of toluene-*p*-sulfonylazetidine with cyclam provides a means for a high yield of the tetra-substituted 3-toluene-sulfonylaminopropane that is a precursor to the macrotricyclic ligands. The complexes formed are principally bimetallic in nature, although the interatomic distances between

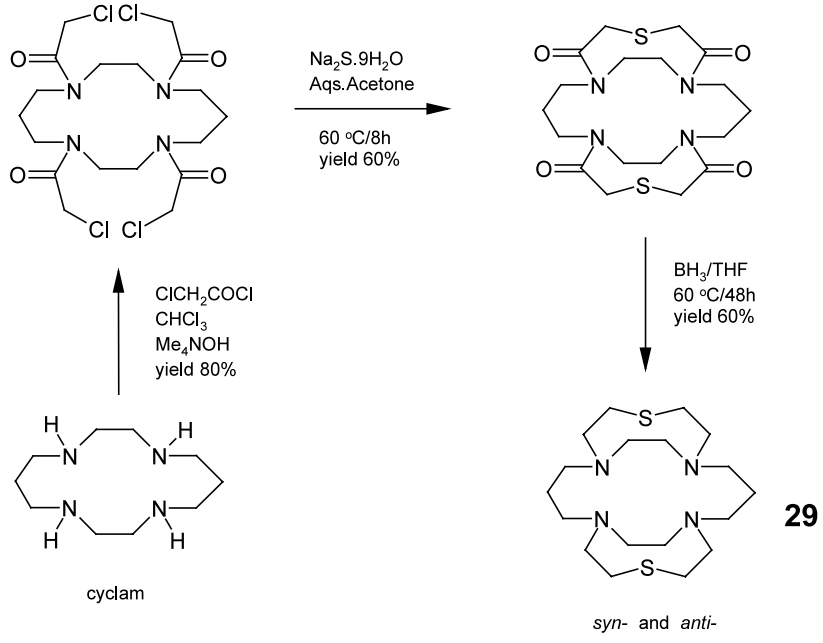

Scheme 7. Synthesis of Ligands **29**.

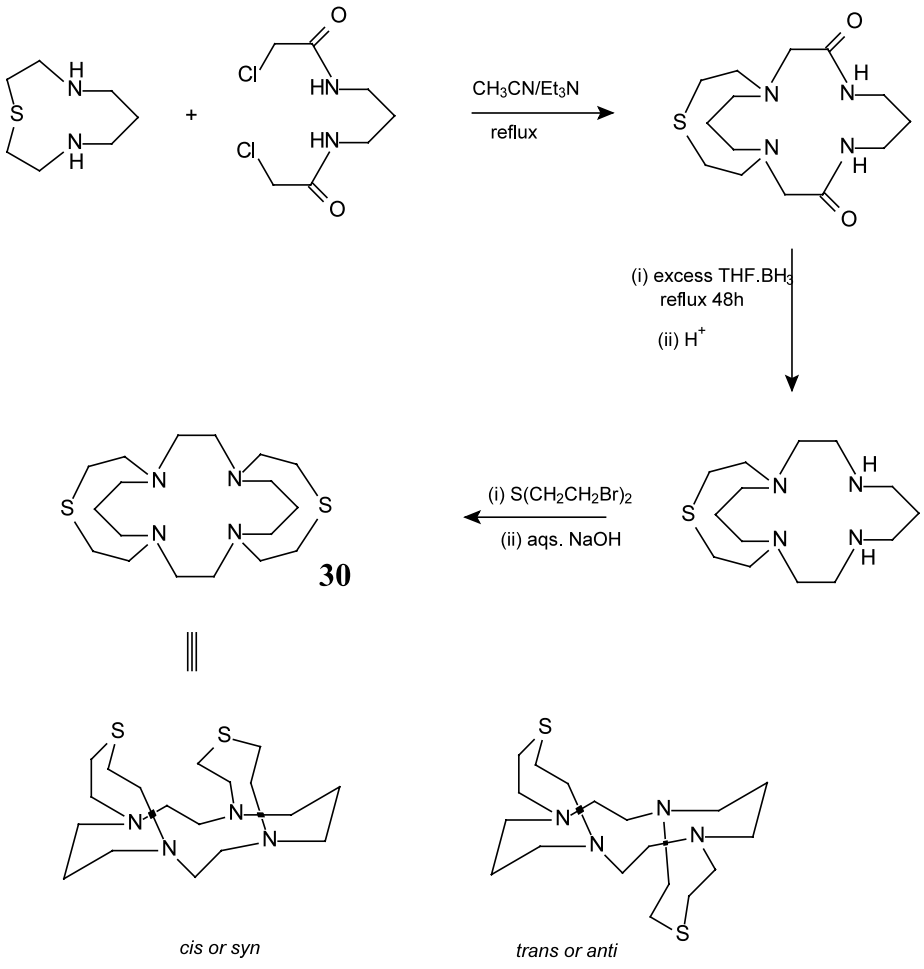

Scheme 8. Synthesis of ligands **30**.

the metal ions are too great to sustain an anionic bridge. 'Reinforced' macrotricyclic ligands with N_2O_2- and N_3O_3- donors have been prepared recently, but no details on metal complexes appear to be available [62].

A protonated tetraaza macrotricycle, $[H(\mathbf{34})]^+$, has been reported [63] in the reaction of 1,5,9-triazacyclodecane with tris-(3-chloropropyl)amine under basic conditions as outlined in Scheme 10.

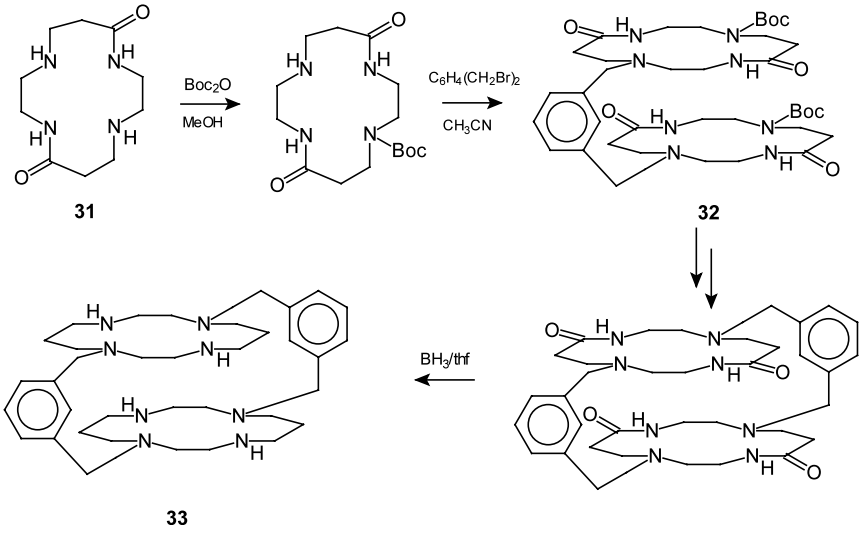

Scheme 9. Synthesis of macrotricycle **33**.

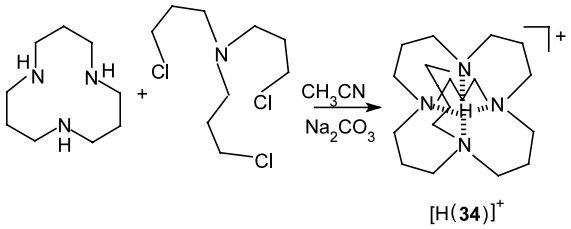

Scheme 10. Synthesis of ion $[H(\mathbf{34})]^+$.

4. Crystal structures

4.1. Protonated species

Structures are available of several protonated forms of macrobicyclic ligands, particularly of smaller ring systems where relatively rare encapsulation of metal ions occurs. In the case of the bicyclic tetraamine **35**, (1, R = H), the ion has been isolated as a triply charged-cation, [34] in which two of the protons are bound to the secondary nitrogens, N1 and N3, and the third acidic hydrogen is localized in a mirror plane between the tertiary centers N2 and N2′. The conformation of the cyclen ring shows elongation along the N1–N3 axis. In contrast, $[H(\mathbf{4})]^+$ is singly protonated at the methylated bridgehead nitrogen [36,37]. In this ion, the N5–H10 bond points almost perpendicular towards the basal molecular plane, owing to repulsions between the methyl groups on N5 and N2. Further protonation does occur, but the second and third steps reveal increasingly weak bases.

The structure of the protonated macrobicycle $[H_4(\mathbf{11})]^{4+}$ (isolated from perchloric acid solution) has been determined [42]. The rings show considerable puckering, and some distortions around the tertiary nitrogens N1 and N2. Unfortunately, owing to considerable disorder in the perchlorate counterions, it was not possible to identify precisely the positions of the protons. However, the ether O lies *exo*- to the tetraazamacrocyclic ring. In the thio analogue, $[H_2(\mathbf{13})]^{2+}$ the ion is less protonated [64] and interestingly, the acidic protons are located one on a secondary nitrogen N3 and the other on the tertiary nitrogen N1. In this instance, the formation of six-membered H-bonded cyclic structures and the minimizing of electrostatic repulsions favor this formation. In this condition, the ligand is conformed to accommodate metal ions without significant alteration. Thus, the *endo* position that the thioether donor adopts is observed in the copper(II) complex of this ligand [53]. These structures contrast markedly with the that of $[H(\mathbf{4})]^+$ where, as noted, only a single proton is taken up. The thioether-analogue of **4** also acts as a proton sponge, and the corresponding oxo-species shows evidence for the H^+ located as a 'quasi metal' complexing agent [65,66].

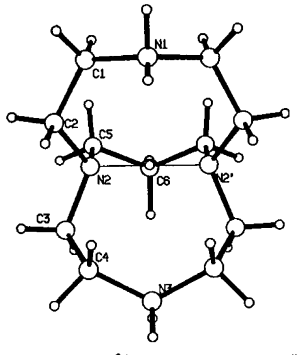

ORTEP diagram of ion $[H_3(\mathbf{35})]^{3+}$.

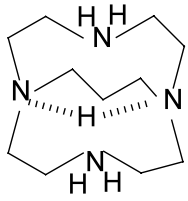

$[H_3(\mathbf{35})]^{3+}$

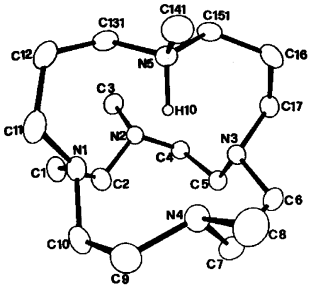

ORTEP diagram of ion $[H(\mathbf{4})]^+$

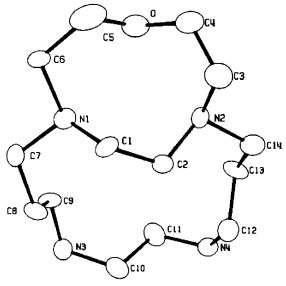

ORTEP diagram of ion $[H_4(\mathbf{11})]^{4+}$

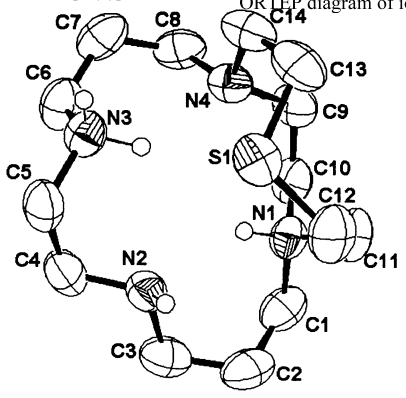

ORTEP diagram of Ion $[H_2(\mathbf{13})]^{2+}$

In the case of macrotricyclic species, there are few examples of protonated crystal structures. The small ion $[H(\mathbf{37})]^+$ was prepared from the protonated bicyclic precursor$[H(\mathbf{36})]^+$ as shown in Scheme 11. The X-ray data [67] shows that the proton in interacts strongly with

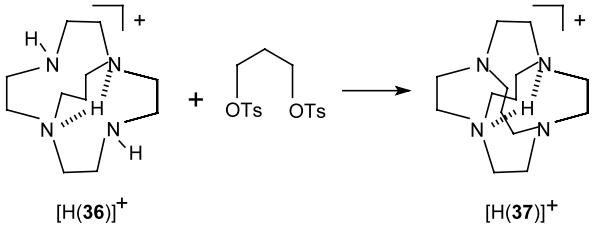

Scheme 11. Synthesis of Ion $[H(\mathbf{37})]^+$.

two bridgehead nitrogen atoms N2 and N4, the N2···H, and N4···H distances being 1.38 and 1.35 Å, respectively. This compares with much weaker interactions with the other two nitrogens N1, and N3 with distances of 2.29 and 2.13 Å, respectively. The fact that the product is $[H(\mathbf{37})]^+$ raises the question whether the proton is encapsulated during or after the formation of the tricycle, although the authors suggest that the ions is formed as shown in Scheme 11. The larger ringed [3[6]] adamanzane cation has also been prepared (Scheme 10), and ^{1}H and ^{13}C-NMR studies provide evidence for a time-averaged D_{2d} symmetry for the cation in solution. In this study, very slow exchange of the inside proton is consistent with a very rigid, yet relatively strainless, cage [63].

The synthesis of the diamide intermediate **26** is shown in Scheme 5. In this instance, there is no protonation of the macrotricycle that appears to show no unexpected strain [67,68]. The C6–C5–O3 angle of 120° is as expected as are the N1–C5 and C5–O3 bond lengths 1.345 and 1.256 Å, respectively. The apical angle, C3–C4–C3′, is lower that expected (114.0°) indicating

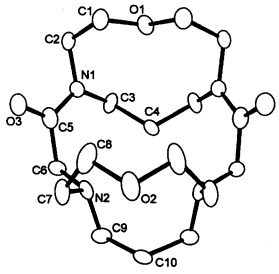

ORTEP diagram of Diamide (**26**)

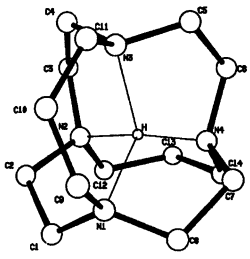

ORTEP diagram of Ion $[H(\mathbf{37})]^+$

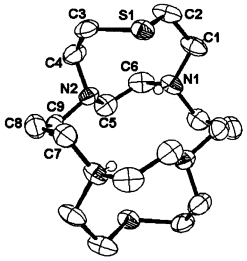

ORTEP diagram of Ion $[H_2(\mathbf{29})]^{2}$

possible strain within the adjacent ten-membered ring.

The structure of the tricyclic ion $[H_2(\mathbf{29})]^{2+}$, has been determined [69]. A center of symmetry is observed, and both thio-ether groups are in *endo* locations. The protons, which point towards the center of the cavity, are located on *trans* tertiary nitrogens presumably to minimize electrostatic repulsion within the ring. This structure represents one of the few examples to date of a tetra-substituted cyclam in which there is a *trans* disposition of the substituents, representing a *trans*-IV conformation of the cyclam ring [58].

4.2. Metal complexes

4.2.1. Macrobicyclic ions

Ligand **4** has been shown to act selectively in the encapsulation of lithium ions [37]. The metal ion sits within a distorted square pyramid and is located 0.85 Å above the basal nitrogen plane, and Li–N bond distances in the range 2.14–2.45 Å are close to those for non-cage aza macrocycles [70]. The complex ions $[Li(\mathbf{19})]^+$ and $[Na(\mathbf{19})]^+$ have been prepared. The structure of the former [47] shows an environment of six nitrogen donors and there is no regular surrounding of the metal ion by the macrobicycle.

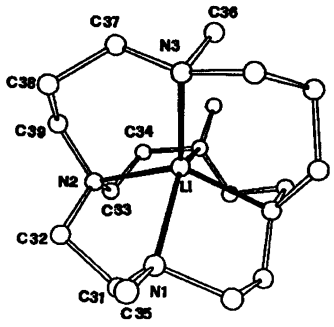

ORTEP diagram of Ion $[Li(\mathbf{4})]^+$

Several metal complexes have been isolated from the sequence of reactions outlined in Scheme 12 where the template method has been employed in the preparation of ligands **11**, **13**, and **15** and X = S is used as an example.

The process represents one of the few successful ring closures of this type at a copper(II) center. It is known that imidates (–N=C–OMe) are prone to hydrolysis, but coordination of the lone pair to the metal ion stabilizes the system such that these ions may be recrystallised from moderately acidic media. The structure of $[Cu(\mathbf{38a})]^{2+}$ (the aza-equivalent of $[Cu(\mathbf{38})]^{2+}$, derived in the preparation of ligand (**16**) [54]) is typical of those refined. The coordination geometry is square pyramidal at copper, and the N5–C11 distance (1.28 Å) is consistent with the double bond character and with the predicted value for an imidate C=N bond (1.282 Å) [70]. Also, at C11, all three angles are 120° within experimental error.

However, at N5, the C11–N5–Cu angle is smaller than expected (114°) while the C11–N5–C12 is larger (127°) reflecting the 'pull' exerted by C10 to allow the formation of the five-membered chelate ring. The C11–O9 distance (1.34 Å) is consistent with its double bond character. In the preparation of (**11**) by this route, (X = O) the amidol complex (–N=C–OH) is first observed,

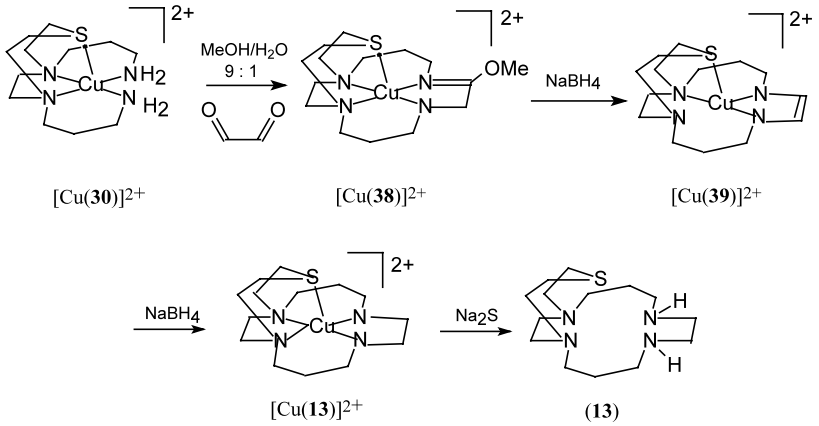

Scheme 12. Synthetic overview to preparation of macrobicyclic ligands.

confirming the formation of hydrated complex ions. The amidol species is tautomeric with an amide in the BH_4^- reduction, and probably derives from the precursor imine-carbinolamine of the type $[Cu(\mathbf{22})]^{2+}$ (Scheme 4). The structure of the ene-amine complex ion, $[Cu(\mathbf{39a})]^{2+}$, (the ether-equivalent of $[Cu(\mathbf{39})]^{2+}$, derived in the synthesis of **11**, [42]) shows a five-coordinate Cu(II) center, although there is a weak interaction (2.98 Å) with one of the perchlorate counter ions. The distance C12–C13 (1.34 Å) confirms the formation of the ene-amine. The bond between the apical oxygen and the metal ion is longer than for the imidate and fully reduced ions for the ether series, and the four macrocyclic nitrogens are most distorted towards a pseudo-tetrahedral arrangement. The copper center is only 0.0325 Å out of the mean plane and the Cu–O vector is 14.8° from orthogonal owing to the tugging of the apical ether donor.

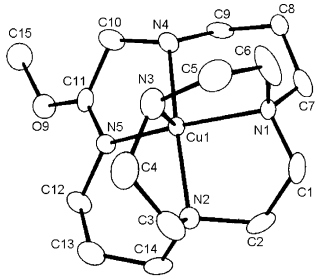

ORTEP Diagram of Ion $[Cu(\mathbf{38a})]^{2+}$

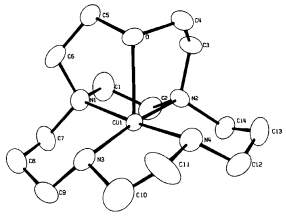

ORTEP Diagram of Ion $[Cu(\mathbf{39a})]^{2+}$

The fully reduced ion, $[Cu(\mathbf{13})]^{2+}$, [53] is representative of the other complexes of this type. The bond lengths and angles are remarkably similar to those of the precursor ion, $[Cu(\mathbf{20})]^{2+}$, (X = NH), indicating that there is no undue strain in the formation of the 14-membered ring. In the non-macrocyclic ion, the four nitrogens are planar within experimental error, and the angle between the apical donor N–Cu vector and the normal to the N_4 plane is 14.5°. This is the result of an inability of the ligand to completely reach over to occupy the apical position completely. In the ion $[Cu(\mathbf{13})]^{2+}$, the closing of the ring reduces the deviation from perpendicularity to 8.2°, but the copper(II) is forced further out of the plane [71] from 0.116 Å in $[Cu(\mathbf{20})]^{2+}$ to 0.141 Å in $[Cu(\mathbf{13})]^{2+}$. The Cu–N bond lengths for the primary ($[Cu(\mathbf{20})]^{2+}$) 2.026 Å and secondary ($[Cu(\mathbf{13})]^{2+}$) 2.025 Å nitrogen atoms are remarkably similar and significantly shorter than the tertiary amines [72].

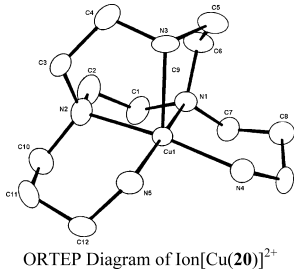

ORTEP Diagram of Ion[$Cu(\mathbf{20})]^{2+}$

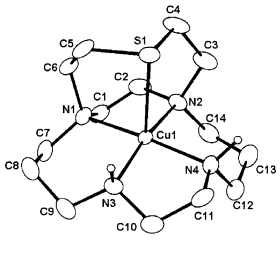

ORTEP Diagram of Ion $[Cu(\mathbf{13})]^{2+}$

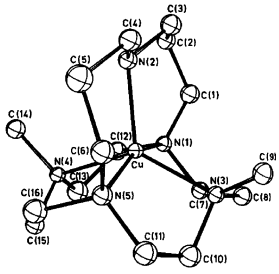

ORTEP Diagram of Ion $[Cu(\mathbf{5})]^{2+}$

It is interesting that in the macrobicyclic complex, the conformation adopted in the cyclam ring is *trans*-1 as shown by the N–H bonds. The structures may be compared with a macrobicyclic complex, $[Cu(\mathbf{5})]^{2+}$, that may be viewed as having an *iso*-cyclam ring bridged by a five atom group containing an apical nitrogen [33]. The features are very similar, with five-coordinate Cu(II) exhibited, and bond lengths almost identical to those provided above. It seems that the ring systems, either cyclam or *iso*cyclam, configure appropriately to suit the optimum geometry of metal ion.

In contrast to the copper(II) ions, the corresponding nickel(II) species exhibit octahedral geometry for the saturated systems. Typical of this class is $[Ni(\mathbf{13})]^{2+}$, where again the *trans*-I conformation is adopted. It is noteworthy that there are few octahedral Ni(II) ions that show this geometry. A detailed analysis of all 14-membered macrocycles

In the Cambridge database [73] shows that the vast majority of *trans*-I species are square planar or square pyramidal and the *trans*-III conformation is associated with octahedral geometry. Also, N-alkylation appears to confer additional thermodynamic stability to the *trans*-I configuration [74]. In the nickel(II) complexes of this type, the Ni–N bond lengths are 2.06–2.07 Å, which may represent a compromise between the calculated M–N distance for *trans*-I cyclam (2.01 Å) [75] and the ideal high-spin Ni(II)–N bond length (2.10 Å) [76]. It would appear that there is a significant increase in stabilization of the kinetic and thermodynamic states owing to the pendant macrocycle. This is supported by the observation that the only successful route to removal of the metal requires the use of Na_2S to promote the deposition of the inert insoluble sulfide. Although the predominant geometry for these macrobicyclic complexes is as shown, a contrast is provided [24] in the complex cation $[Ni(\mathbf{40})(NCMe)]^{2+}$. In this ion, one of the pendant arms is located out of the equatorial plane, occupying rather an axial site, with the acetonitrile solvent coordinated equatorially.

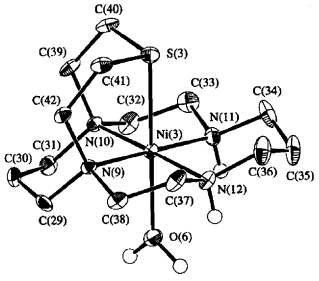

ORTEP Diagram of $[Ni(\mathbf{15})(OH_2)]^{2+}$

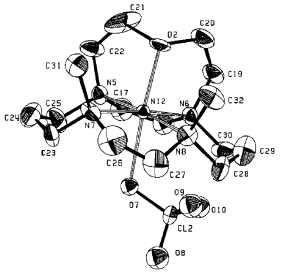

ORTEP Diagram of $[Ni(\mathbf{41})(OClO_3)]^{+}$

This results in two different sets of Ni–N distances, with N2 and N4 at a mean distance of 2.13 Å and the remaining bonds at 2.07 Å. Octahedral geometry is maintained in the ions $[Ni(\mathbf{40})(NCMe)]^{2+}$] and $[Ni(\mathbf{15})(OH_2)]^{2+}$. The latter is observed as part of a much more complex system, $[Ni(\mathbf{15})(ClO_4)](ClO_4)\cdot 2[Ni(\mathbf{15})(OH_2)](ClO_4)_2\cdot 6H_2O$ unlike that seen in any of the copper analogues. A detailed crystal structure has provided evidence for three independent ions (including one $[Ni(\mathbf{15})(OClO_3)]^{2+}$ ion and a two forms of $[Ni(\mathbf{15})(OH_2)]^{2+}$) found in the lattice [77]. In addition, after prolonged standing, a yellow form of the perchlorato complex has also been isolated. (In this case, it is assumed that the thioether group is now *exo* and a square planar form of the ion is obtained). As is seen in the diagram, the isomeric form of the ligand **15** permits the formation of a *trans*-III conformation. Similar structures are found for the other ions in the lattice, and although all the Ni–S distances are identical at 2.39 Å, each of the two aqua ions has a slightly longer Ni–S bond length (2.42 Å) implying that a small *trans* effect exists for aqua vs. perchlorato coordination in the sixth site. The metal center and the N_4 framework are virtually coplanar, but the Ni–N tertiary bond distances are 2.105 and 2.113 Å close to the ideal high-spin value. The implication is that the cyclam ring has expanded to accommodate the nickel ion. In addition, the pendant ring can now overlap the metal center better, such that the Ni–S vector is tilted 5.7° towards the tertiary nitrogens, less than that for the complexes where the pendant group is in a nine-membered ring.

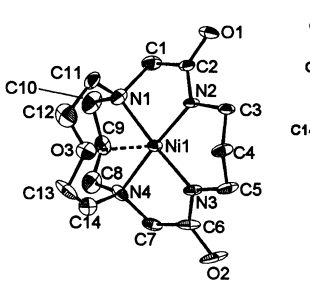

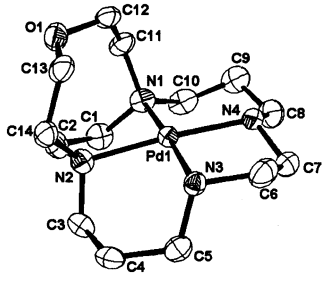

ORTEP Diagram of $[Ni(HL(\mathbf{20})]^{+}$ ORTEP Diagram of $[Pd(\mathbf{11})]^{2+}$

As described earlier, the octahedral complex ions adopt a *trans*-I conformation of the cyclam ring. In an attempt to assess the extent of a possible conformational change, the di-methylated ligand, **41**, was synthesized providing a macrocyclic ring with only tertiary donors, and the nickel(II) ion prepared [78]. Two unique ions were found in the lattice both of which exhibit a *trans*-I conformation. The ring appears to adjust bond-length changes to accommodate possible crowding. In both ions, (see $[Ni(\mathbf{41})(OClO_3]^{+}$) the N7–C26 and N8–C27 distances are extended (mean 1.59 Å) and the C26–C27 contracts (1.41 Å). However, all Ni–N bonds lie in the range 2.10–2.12 Å as anticipated for high-spin nickel(II).

As will be discussed, there are significant differences in the UV–vis spectra and electrochemistry of the $[Ni(\mathbf{12})]^{2+}$and $[Ni(\mathbf{14})]^{2+}$ ions. However, to date, no crystal structures of these ions are yet available.

Square planar complexes of macrobicycles have been identified [41]. In the complex ion $[Ni(HL(\mathbf{20})]^{+}$, based upon the diamide ligand described earlier, at the pH used for isolation of the species, one of the amide residues is deprotonated, leading to an complex ion of single charge. Owing to the strong ligand field imposed by the bis-amide, the resulting structure is planar, with weak interactions observed between the Ni and the apical O3 (Ni–O3 = 2.651 Å) and an oxygen atom of an adjacent ligand (Ni–O3a = 2.451 Å). The metal ion lies

in the plane of the four N-donors, but the Ni–O3 vector is 13° from perpendicular, substantially greater than in $[Ni(\mathbf{8})(OClO_3)]^+$ (deviation 5.5°). Also, the vector to atom O3a located on a neighboring ligand, is 8.2° from normal, creating a zig-zag pattern throughout the lattice. A square planar nickel(II) ion configuration is adopted in $[Ni(\mathbf{11})(PF_6)]^+$ [45], although there is a very weak interaction with one of the fluorides of the PF_6^- counter ion.

In contrast to the thioether ligand species, $[Pd(\mathbf{13})]^{2+}$, which has an *endo*- structure similar to the protonated ion described above, the corresponding ether ion, $[Pd(\mathbf{11})]^{2+}$, adopts an *exo*-representation of the pendant ring [64], leading to the square planar ion shown. Tertiary (2.075 Å) and secondary (2.045 Å) nitrogen bonds to the metal ion are consistent with previous observations, and the non-bonding Pd–O5 distance (3.4 Å) is similar to that observed in the $[Pd(9N_3)]_2^{2+}$ ion, ($9N_3$ = 1,4,7-triazacyclononane) that also exhibits[79] the *exo*- form of the nine-membered ring.

Cobalt(III) has also been complexed to ligand **8** [80]. In this ion, there is almost complete overlap (Cl(1)–Co(1)–O(1) = 178.53 (22)° of the pendant ring with respect to the metal ion. As is seen in Table 1, the cobalt(III)- coordinate bonds are similar to those expected for an octahedral complex ion of this type, and the Co–O bond quite short. The cobalt ion lies below the mean plane of the N_4 donors, away from the ether, consistent with the greater electronegativity of the chloride.

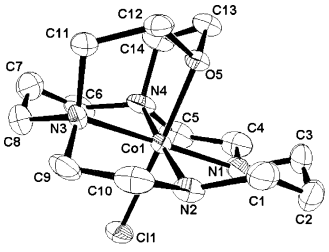

ORTEP of Ion $[Co(\mathbf{8})(Cl)]^{2+}$

The macrobicyclic ligand, **42**, has been synthesized [36] and the cobalt(III) complex prepared. In this ion, the carbonato ligand occupies adjacent sites as expected, leading to a *cis*-configuration of the ligand. The N1–Co–N3 angle is 176.8°, indicating that the ligand adjusts to meet the octahedral requirements of the d^6 ion. Also, the two six-membered rings containing N1 are in a twist-boat conformation, whereas the chair form is observed in the other three rings. This configuration is also that adopted in the corresponding nickel(II) ion $[Ni(\mathbf{42})(NO_3)]^+$ [81].

Table 1
Selected interatomic distances (Å) and bond angles (°) for $[Co(8)Cl](ClO_4)_2$

Bond distances			
Co(1)–Cl(1)	2.219(3)	Co(1)–N(2)	2.007(9)
Co(1)–O(1)	1.924(6)	Co(1)–N(3)	1.949(9)
Co(1)–N(1)	1.979(9)	Co(1)–N(4)	1.978(8)
Bond angles			
Cl(1)–Co(1)–O(1)	178.53(22)	O(1)–Co(1)–N(4)	92.6(3)
Cl(1)–Co(1)–N(1)	92.5(3)	N(1)–Co(1)–N(2)	96.5(5)

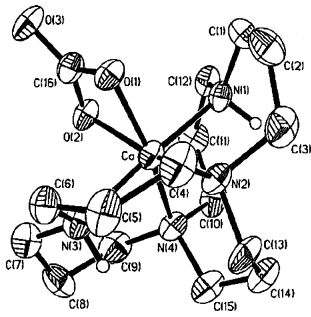

ORTEP Diagram of Ion $[Co(\mathbf{42})(CO_3)]^+$

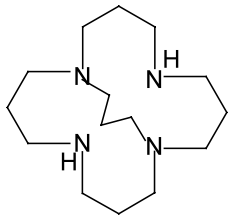

(**42**)

A europium(III) cryptate complex has been prepared by the reaction of aqueous Eu^{3+} with $[Na(\mathbf{18})]^+$ at 60°. The crystal structure [46] shows the metal encapsulated within the cryptate coordinated by the four dipyridyl nitrogen donors and the two bridgehead nitrogens. The polyamine chain is not involved in the bonding, and nine-coordination around the metal ion is completed by three chlorides. The structures of three lanthanide ions containing ligand **43** have been determined [82]. All eight nitrogen donors are involved in the complexation, and there are two open faces presented by the macrobicycle that are filled by either chloride ion or water molecules to accommodate the coordination requirements of the lanthanides.

4.2.2. Macrotricyclic ions

There are significantly fewer examples of crystal structures of these systems.

In the macrotricyclic complex $[HLi(\mathbf{29})](ClO_4)_2$, the lithium is two-coordinate [69] but is located within the plane of the cyclam ring. The proton is disordered between two centro-symmetrically related N-atoms and one of these contributors is shown in the ORTEP diagram. As seen previously, the thio-ethers are extended over the cyclam macrocycle.

In the ion $[Cu(\mathbf{28})]^{2+}$, two forms of the complex are found within the lattice, comprising 5- and 6- coordinate copper(II), respectively. This ligand cannot adopt a *trans*-III form of the cyclam ring, and both nine-membered pendant rings are located on the same side of the macrocycle [56]. Representations of the cations are presented. In the five-coordinate ion, (**28a**), the Cu–N bond distances, Cu1–N102 2.076(9) and Cu1–N102 2.076(9) Å are somewhat longer than the corresponding

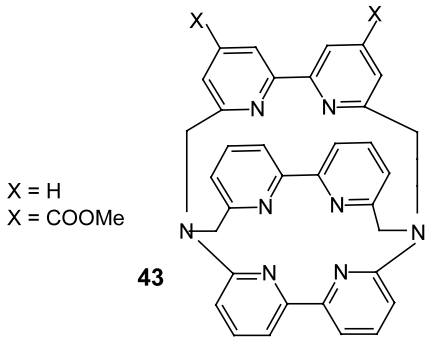

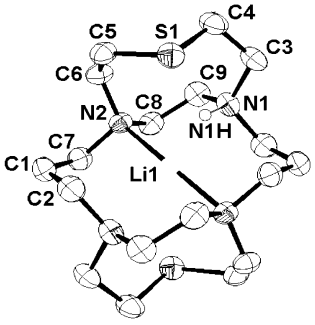

ORTEP Diagram of Ion $[HLi(\mathbf{29})]^{2+}$

distances in the macrobicyclic complex ion $[Cu(\mathbf{11})]^{2+}$. But the Cu–O distance is identical Cu1–O101 = 2.276(11) (2.275(9) Å. The angle N101–Cu1–N101a = 160.9(3)° suggests some distortion in the macrocycle confirmed by the angles N101a–Cu1–N102 = 96.0(4), N101a–Cu1–N102a = 83.9(4)°.

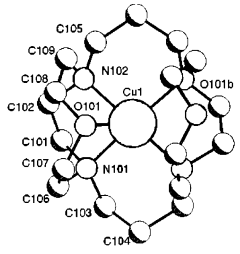

Crystallographic diagram of $[Cu(\mathbf{28})a]^{2+}$

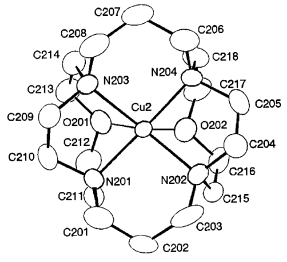

Crystallographic diagram of $[Cu(\mathbf{28})b]^{2+}$

However, in the six-coordinate ion, there is much greater asymmetry with a large variation in bond lengths: Cu2–N201, 2.082(7), Cu2–N202, 2.096(7), Cu2–N203, 2.103(7), Cu2–N204, 2.068(7), Cu2–O201, 2.597(7), Cu2–O202, 2.427(7) Å. Corresponding angles are: N201–Cu2–N202, 93.9(3), N201–Cu2–N204, 75.6(3), N202–Cu2–N203, 160.6(3)°.

A preliminary structure of $[Cu(\mathbf{27})]^{2+}$ is also available [56]. In this ion, there is the possibility of a *trans*-I disposition of the rings, and as seen in the nickel(II) structures of **8** and **15**. However, the predominance of five-coordination at the metal ion appears to take precedence, with both rings again on the same side of the cyclam ring. The Cu–N bond lengths are all fairly similar (2.075 Å), with the exception of Cu–N4 (2.119 Å). There is again a lack of planarity with angles N2–Cu–N4 162.07°, and N1–Cu–N2 87.02°. The Cu–O11 distance is 2.31 Å, with the other oxygen at a non-bonding distance.

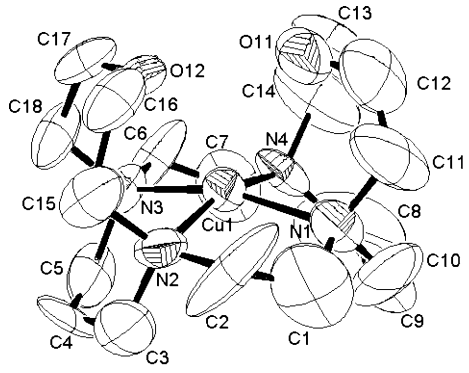

ORTEP Diagram of Ion $[Cu(\mathbf{27})]^{2+}$

As indicated earlier, ligand **29** can exist in *syn*- and *anti*- forms, but in the synthesis, relatively small amounts of the latter conformation are formed. However, it appears that the intermediate Li^+ and protonated complexes display greater *trans* ratios. Nickel(II) complexes have been isolated [59], and their structures determined. In the *syn*- form, $[Ni(\mathbf{29b})]^{2+}$, the cyclam adopts an octahedral *cis*- configuration. In the crystal, the Ni–N1 and Ni–N3 bond distances are similar, 2.172(8) Å and likewise the Ni–N2 and Ni–N4 2.100(1) Å, with the Ni–S1 and Ni–S2 values 2.451 and 2.427 Å, respectively. Bond angles are also in pairs, with N2–Ni–N1 = 84.3° and N4–Ni–N3 = 93.7°. The other isomer, $[Ni(\mathbf{29a})]^{2+}$, is somewhat more symmetrical, with bond angles N2–Ni–S1 = 98.6° and N1–Ni–S1 = 81.1°, and displays the very unusual *trans*-IV conformation of the cyclam ring. This isomer is octahedral and the Ni–N bond lengths (2.125(2) Å) are consistent with those (2.100(2) Å) reported earlier [84] for octahedral $[NiN_6]^{2+}$ ions. Ion $[Ni(\mathbf{29a})]^{2+}$ may be compared with the complex ion $[Ni(9\text{-}N_2S)_2]^{2+}$ (9-N_2S = 1,4-diaza-4-thio-nonane) that has a similar octahedral N_4S_2 donor environment, but with no constraining side arms of the ring. The average Ni–N bond length in $[Ni(9\text{-}N_2S)_2]^{2+}$ is (2.109(1) Å), while the Ni–S bond is 2.418 Å. The average five-membered intra-ligand angles, S–Ni–N, (85.1°) and N–Ni–N (80.5°) [85] differ significantly from those in the macrotricyclic ion. Although the N1–Ni–N1′, N2–Ni–N2′ and S1–Ni–S1′ intra-ring angles are all 180(3)°, the corresponding values for the intra-ring angles are S–Ni-N1, (81.1°) and N2–Ni–N1 (96.5°) probably reflect increased constraints within the individual nine-membered rings when they constitute part of the macrotricyclic cage.

The copper(II) ion $[Cu(\mathbf{29})]^{2+}$ has also been studied. In this case, the configuration is best described as a five-coordinate distorted square pyramid [58]. The configuration is of N_3S_2 character, with one of the nitrogen atoms non-bonding. The Cu–S bond distances are

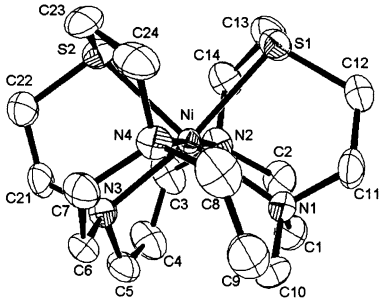

ORTEP Diagram of Ion $[Ni(\mathbf{29}b)]^{2+}$

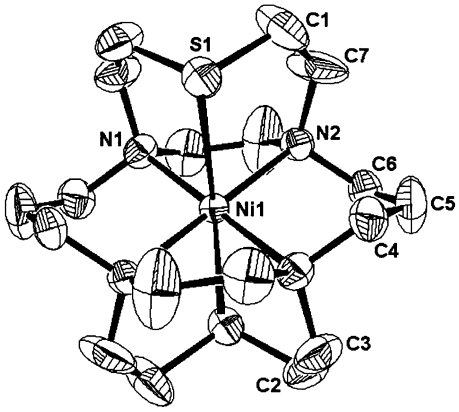

ORTEP Diagram of Ion $[Ni(\mathbf{29}a)]^{2+}$

Cu1–S1 = 2.68 and Cu1–S2 = 2.55 Å, the latter similar to that in $[Cu(\mathbf{13})]^{2+}$. The elongation of one of the Cu–S bonds may suggest a tendency towards a tetrahedral ion, although the prevalence of five-coordination in copper(II) systems has been featured in this report.

The synthesis and crystal structure of the nickel(II) complex of ligand (**44**) have been reported [23]. The

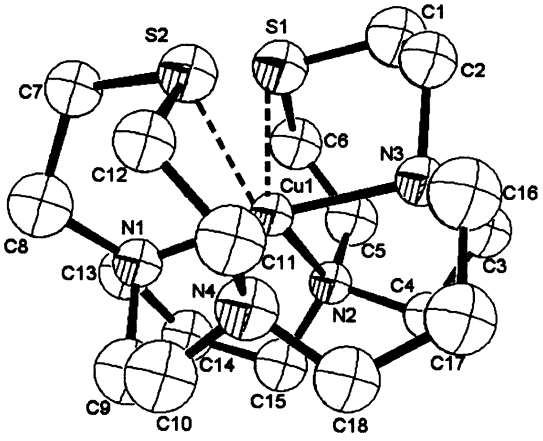

reaction of nickel(II) with tris(aminoethyl)amine in the presence of formaldehyde results in the novel complex ion in which two saturated 1,3,6,9-tetraazacyclodecane rings are linked face to face by two ethylene bridges. The disposition of the rings is *anti*-parallel.

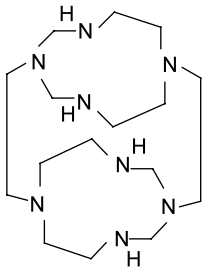

Ligand **44**

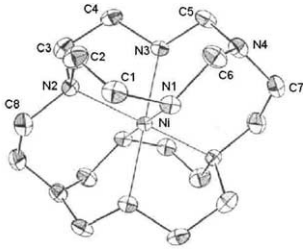

$[Ni(\mathbf{44})]^{2+}$

5. Solution chemistry and reactions

Several investigations have been made regarding the ability of some of the cages to accommodate protons and lithium ions. The macrobicycle, 1, is a potent proton sponge, (concentration $pK_1 > 15$, pK_2 7.242 and pK_3 3.202), being a stronger base in water than hydroxide ion [35]. Attempts were made to replace the proton by Li^+, but reaction of $[H_3(1)]^{3+}$ with Li^+ in 1 M NaOH showed no sign of replacement after heating to 100 °C for 1.5 h. The cage 4 encapsulates Li^+ selectively with no evidence for coordination with Na^+ or K^+, although Zn^{2+} is incorporated. By use of ^{13}C and ^{7}Li-NMR, the time taken to reach equilibrium $Li^+_q + 4_{aq} \leftrightarrow [Li4]^+_{aq}$ (4, 0.5 M in 0.2 M KOH, Li^+, 0.05 M LiOH) was determined to be about 50 min, and the equilibrium constant is greater than 10^3 M. Thermodynamic consequences of the reaction have been described [37]. The inertness of $[H(\mathbf{37})]^+$ has also been determined potentiometrically [67] The ion is aprotic in the range pH 0–14, lack of reaction over 1 month in 1 M NaOD is consistent with a rate constant of $< 2 \times 10^{-8}\ s^{-1}$ under these conditions. Similar observations have been made [62] (proton dissociation rate 0.1 M NaOD, 25°, $< 4 \times 10^{-8}\ s^{-1}$) for ion $[H(\mathbf{34})]^+$. The metal ion $[Ni(\mathbf{44})]^{2+}$ is particularly inert towards substitution for a complex of this metal, being stable to ligand substitution with CN^-, even in boiling water.

Many of the metal complexes reported herein are redox active, and have been the subject of more extensive coverage in the literature cited. However, it is useful to identify less commonly observed highlights, and some details of ions of less common oxidation states that have sufficient kinetic and thermodynamic stability to be addressed in terms of kinetic and spectroscopic studies.

An interesting feature in the template syntheses involving the Cu(II) ions [53,54] is the characterization of an unusual imidate complex, formed with a stoichiometric deficiency of BH_4^-. As indicated, the oxygen and nitrogen analogues of which have been characterized crystallographically. It was also observed that the addition of base to an equilibrium mixture of complexes $[Cu(\mathbf{21})]^{2+}$ and $[Cu(\mathbf{22})]^{2+}$ (Scheme 4) led to the mono-amidoN_5 macrobicylic ligand (Scheme 13). This is the first example of the formation of a mono-amide from a condensation reaction between a diamine and glyoxal. That the imine-carbinolamine ($[Cu(\mathbf{22})]^{2+}$) should undergo such a base catalyzed proton shift is supported by the fact that ionization of methylene protons adjacent to an imine in a five-membered ring is well-documented [83]. The resulting enol then undergoes a tautomeric proton shift to form the amide $[Cu(\mathbf{46})]^{2+}$. During the synthesis of **11**, **13**, and **16**, the amide species was formed in quantity under basic conditions suggesting that the mechanism of the glyoxal condensation is common to all three systems. A unique feature of these syntheses is the formation under basic conditions of bicyclic monoamides **46**, species that are difficult to prepare under other circumstances.

Macrobicyclic and macrotricyclic nickel(II) complexes, Table 2, exhibit UV–vis spectra characteristic of octahedral systems. Differences relate principally to ions of lower symmetry accompanied by higher extinction coefficients. There is a remarkable similarity in the spectra of the macrobicyclic metal complex ions. This is true particularly for the copper(II) ions. Notable exceptions are the 'hemi-cryptate' complexes of ligands **12** and **14**. For example, in the Cu(II) ions containing ligands **13**, **14** and **15**, there is a significant new absorbance at 330 nm and a shift of 70 nm in the 530 peak. The effect appears to be less significant in the nickel ion with ether donors, possibly owing to the relatively easy displacement of the ether O by solvent.

The spectra of $[Cu(\mathbf{8})]^{2+}$ and $[Cu(\mathbf{11})]^{2+}$ are very similar, as are those of $[Cu(\mathbf{13})]^{2+}$ and $[Cu(\mathbf{15})]^{2+}$. This implies that there is no significant variation in the solution state geometries of the two isomers. This result is somewhat surprising given that the solid state structures were *trans*-III and *trans*-I for the $[Cu(\mathbf{13})]^{2+}$ and $[Cu(\mathbf{15})]^{2+}$, respectively. Even if these structural differences are maintained in solution, they do not appear to cause significant perturbations of the ligand fields. This result is, however, in agreement with the prediction that both the (**13**) and (**15**) are sufficiently flexible that they do not alter the bonding requirements of the copper(II) center relative to each other.

Table 2
UV–vis data

Complex	λ_{max} (nm) (ε (M^{-1} cm^{-1})
Nickel(II) complexes	
$[Ni(\mathbf{8})(OH_2)]^{2+}$	197 (6100), 334 (11), 505 (6), 675 (3), 1059 (3).
$[Ni(\mathbf{15})]^{2+}$ [a]	390(sh), 481 (8), 940 (8)
$[Ni(\mathbf{11})(OH_2)]^{2+}$	222 (2420), 337(17), 515(10), 681(5)
$[Ni(\mathbf{16}(OH_2)]^{2+}$	331 (14.5), 510 (9), 920 (12.5)
$[Ni(\mathbf{12})(OH_2)]^{2+}$	339(7), 520 (5), 1077 (3)
$[Ni(\mathbf{13})(OH_2)]^{2+}$	261 (1900), 504 (14), 1020 (18)
$[Ni(\mathbf{14})(OH_2)]^{2+}$	355(sh), 544(18), 817(5)
$[Ni(\mathbf{15})(OH_2)]^{2+}$	205 (1800), 498 (11), 685 (7), 848 (9), 989 (18)
$[Ni(\mathbf{29a})]^{2+}$	295 (5550), 522 (12), 663 (9.4), 902 (9), 996 (9.5)
$[Ni(\mathbf{29b})]^{2+}$	278 (506), 538 (16.4), 869 (25), 907 (31), 998 (26)
$Ni[(9\text{-}N_2S)_2]^{2+}$	350, 548, 854, 930
$[Ni(\mathbf{11})(OH_2)]^{3+}$	261 (6600), 326(sh)(4900), 374(5300), 634(37)
$[Ni(\mathbf{16})(OH_2)]^{3+}$	303 ($1.06x10^4$), 380 (sh), 665 (37)
$[Ni(\mathbf{16})(F)]^{2+}$	279 (8000), 343 (7100), 683 (35)
$[Ni(\mathbf{12})(OH_2)]^{3+}$	317 (2160), 394 (1440)
$[Ni(\mathbf{8})(OH_2)]^{3+}$	315 (3700), 390 (3000)
Copper(II) complexes	
$[Cu(\mathbf{15})]^{2+}$	286 (4600), 533 (135), 743 (32)
$[Cu(\mathbf{14})]^{2+}$	282 (3200), 312 (4620), 603 (352)
$[Cu(\mathbf{13})]^{2+}$	281 (5400), 532 (143), 728 (37)
$[Cu(\mathbf{11})]^{2+}$	274 (6800), 522 (102)
$[Cu(\mathbf{16})]^{2+}$	276 (5700), 567 (145), 859 (42)
$[Cu(\mathbf{8})]^{2+}$	278 (6555), 520 (114), 622(28)

Aqueous solution.
[a] Yellow, square planar form, see text.

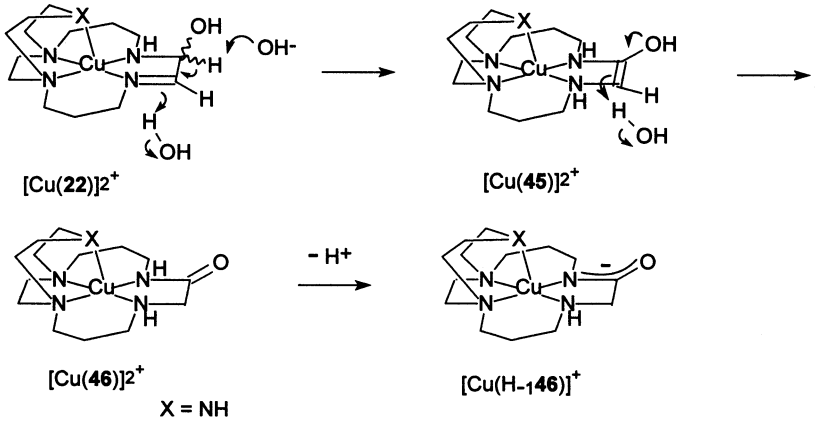

Scheme 13. Base hydrolysis of ion $[Cu(\mathbf{22})]^{2+}$ leading to a mono-amide complex.

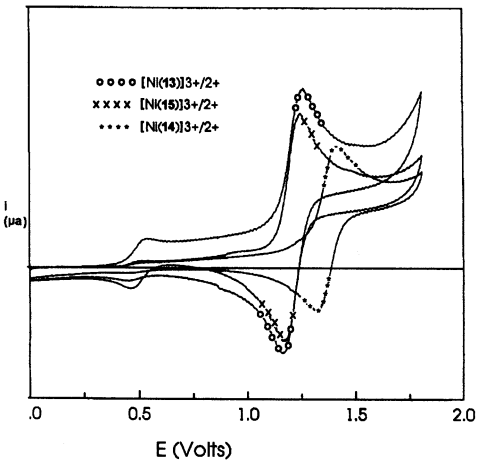

Fig. 1. CV curves of Ni(II) macrobicyclic complexes.

The nickel(II) ions show redox behavior, yielding both Ni(I) and Ni(III) in electrochemical experiments. In general, the spread between the two oxidation states is about 2 V, the Ni(III) ions acting as strong oxidants. In general, the Ni(III) state is more accessible for study, being sufficiently stable in acidic media for kinetic studies to be undertaken. Cyclic voltammetric studies generally show at least quasi-reversibility, as is seen in Fig. 1 for the Ni(II)/(III) couples of ligands **13**, **14** and **15**.

In this figure, the couple for ferrocene–ferrocinium is also shown as a marker. The differences already noted in the behavior of the much less symmetric hemicryptate ion $[Ni(\mathbf{14})]^{3+/2+}$ are again evident in the increase of ca. 70 mV in the redox potential.

5.1. EPR spectroscopy

Being a low spin d^7 ion, nickel(III) is readily characterized by epr at 77 K. In general the split between $g_{||} \sim 2.03$ and $g_{\perp} \sim 2.2$ is observed, owing to Jahn–Teller distortion of the ion. Fig. 2 provides examples of ions of the macrobicyclic complexes, where the coordination of variou anions and other donors in the axial position is

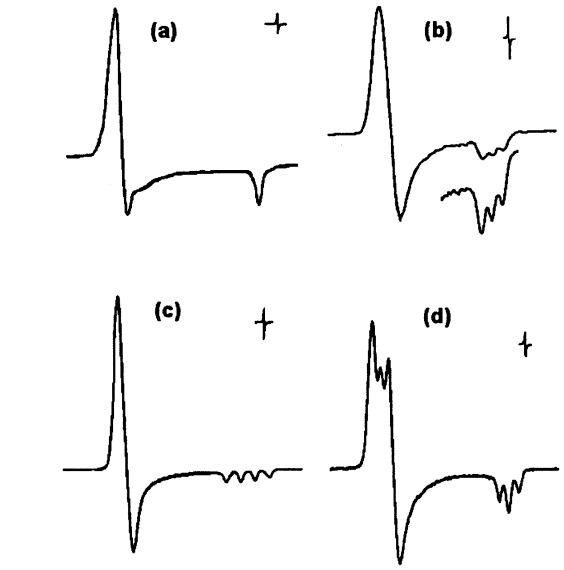

Fig. 2. Epr spectra of Ni(III) complexes in frozen matrices: (a) $[Ni(\mathbf{11})(OH_2)]^{3+}$ (aq); (b) $[Ni(\mathbf{16})(OH_2)]^{3+}$ (aq); (c) $[Ni(\mathbf{11})(Cl)]^{2+}$ (MeCN); (d) $[Ni(\mathbf{11})(NO)]^{3+}$ ($MeNO_2$).

consistent with the hyperfine interactions. Oxidation of [Ni(**15**)(SCN)](SCN) yielded a spectrum in which the $g_{||}$ feature was a triplet ($A_{||} = 19$ G), consistent with the presence of a mono-thiocyanato complex in which the axial thioether remained coordinated.

Typical of the copper(II) (d^9) spectra is that at room-temperature (aqueous solution) where the spectrum of $[Cu(\mathbf{15})]^{2+}$ is isotropic, with $g_{iso} = 2.090$, with four lines due to hyperfine splitting ($A_{iso}^{Cu} = 85.4$ G; $^{63,65}Cu$, $I = 3/2$) [63]. The frozen solution (77 K, 1:1 DMF:CH_3CN) spectrum is consistent with axial symmetry with $g_{||} = 2.203 > g_{\perp} = 2.059$ indicative of a tetragonally elongated (Jahn Teller effect) geometry with the unpaired electron predominantly in the $d_{x^2-y^2}$ orbital. These values are similar to those of other similar macrobicyclic complexes and of $[Cu(cyclam)]^{2+}$ and reflect the predominance of the equatorial cyclam ring in the $[Cu(\mathbf{15})]^{2+}$ species.

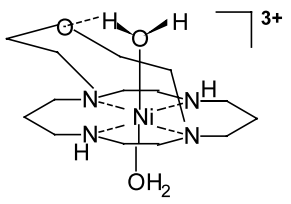

$[Ni(\mathbf{12})(OH_2)_2]^{3+}$

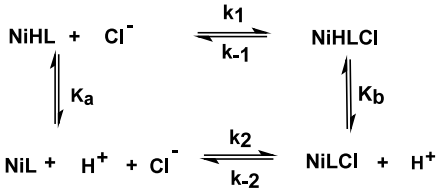

Kinetic studies have been made on the substitution at Ni(III) for the series containing ligands **8**, **11**, and **12** [41,45]. A feature of these studies is the presence of an acid–base equilibrium not observed in the corresponding $[Ni(III)(cyclam)]^{3+}$ kinetics. It is suggested that there is an equilibrium that involves an ion of the type $[Ni(\mathbf{12})(OH_2)_2]^{3+}$ in which there is detachment of the axial O donor and its replacement by a water molecule.

In the reaction with chloride, the rate law derived from this equilibrium set may be represented as:

$$k_{obs} = (k_1[H^+] + k_2K_a)[Cl^-]/(K_a + [H^+]) + (k_{-1}[H^+] + k_{-2}K_b)/(K_b + [H^+])$$

and is more complex than that observed for the reaction of $[Ni(III)(cyclam)]^{3+}$ with chloride [86] under the same conditions.

The enhanced acidity of coordinated water is well known, and, at lower acid concentrations, the presence of a lone pair on the ether provides a template for formation of a hydrogen bond with the incoming water molecule as shown. This interaction has the effect of increasing the ability of the coordinated water to donate electrons to the nickel(III) thus labilizing the complex. At higher hydrogen ion levels, the ether group preferentially H-bonds to the H_3O^+ present in solution leaving the isolated water bound to the Ni(III) which in turn becomes more inert towards substitution. Substitution rates are of the order of 10^2–10^3 M^{-1} s^{-1} for reaction with chloride ion [45]. Further studies on these systems in aprotic solvents where acid–base equilibria are not effective will provide more data on the substitution processes at these ions with a less common oxidation state.

Redox reactions of the mono-aquo- and chloro-macrobicyclic Ni(II)/(III) complexes with the outer sphere reagent $[Ni(9\text{-}aneN_3)_2]^{2+/3+}$ have also been investigated [25].

Lanthanide complexes are known to exhibit luminescence. Recently, [46] the emission of the europium(III) complex of **17** has been examined, where it is observed that the luminescence is modulated by pH, owing to sequential protonation within the polyamine chain located as a bridge between the dipyridyl units of the ligand.

6. Concluding comments

The availability of macrobicyclic and macrotricyclic ligands is providing a rich source of new chemistry, particularly in view of the wide variety of metal ions that can be incorporated into the ligand framework. Much remains to be explored in determining the unique role the ligands must play in the reactivity of these species, but the stabilizing of less common oxidation states, the sequestration of protons, the mixtures of donors possible and the variation of geometries of the metal ions will certainly lead to new and interesting observations.

Acknowledgements

A.McA wishes to acknowledge, with thanks, his co-authors whose skills have made possible many of the ligand syntheses outlined in this review. Much of their work is currently in preparation for submission for publication. Thanks are also due to crystallographers Tosha Barclay, Kathy Beveridge and Mike Zaworotko whose help has been invaluable. The support of NSERC is gratefully acknowledged.

References

[1] N.F. Curtis, J. Chem. Soc. (1960) 4409.
[2] N.F. Curtis, D.A. House, Chem. Ind. (1961) 1708.
[3] (a) M.C. Thompson, D.H. Busch, Chem. Eng. News 17 (1962) 57; (b) M.C. Thompson, D.H. Busch, J. Am. Chem. Soc. 86 (1964) 3651.
[4] D.H. Busch, K. Farmery, V. Goedken, A.C. Katovic, A.C. Melnyk, C. Sperati, N. Tokel, Adv. Chem. Ser. 100 (1971) 44.
[5] G.A. Melson (Ed.), Coordination Chemistry of Macrocyclic Compounds, Plenum Press, New York, 1979.
[6] I. Bertini, I.H.B. Gray, S.J. Lippard, J.S. Valentine (Eds.), Bioinorganic Chemistry, University Science Books, Mill Valley, CA, 1994.
[7] R.W. Hay, Bio-Inorganic Chemistry, Ellis Horwood Limited, Chichester, 1984.
[8] G. Wilkinson (Ed.), Comprehensive Coordination Chemistry: The Synthesis, Reactions, Properties and Applications of Coordination Compounds, vol. 1–7, Permagon Press, Oxford, 1987.
[9] L. Lindoy (Ed.), The Chemistry of Macrocyclic Ligand Complexes, University Press, Cambridge, 1989.
[10] A. Bianchi, M. Micheloni, P. Paoletti, Coord. Chem. Rev. 110 (1991) 17.
[11] E. Kimura, T. Koike, Comments Inorg. Chem. 11 (1991) 285.
[12] D.H. Busch, N.W. Alcock, Chem. Rev. 94 (1994) 585.
[13] M. Mitewa, P.R. Bontchev, Coord. Chem. Rev. 135 (1994) 129.
[14] J.P. Danks, N.R. Champness, M. Schröder, Coord. Chem Rev. 174 (1998) 417.
[15] G.W. Franklin, D.P. Riley, W.L. Neumann, Coord. Chem. Rev. 174 (1998) 133.
[16] A. McAuley, S. Subramanian, Coord. Chem Rev. 200–202 (2000) 75.
[17] P.V. Bernhardt and E.J. Hayes, J. Chem. Soc. Dalton Trans., (1998) 3539.
[18] P.V. Bernhardt, Inorg. Chem. 38 (1999) 3481.
[19] P.V. Bernhardt, L.A. Jones, J. Chem. Soc. Chem. Commun. (1997) 655.
[20] (a) A.M. Sargeson, Coord. Chem. Rev. 151 (1996) 89; (b) N.M. Di Bartolo, A.M. Sargeson, T.M. Donlevy, S.V. Smith, J. Chem. Soc. Dalton Trans, (2001) 2303.
[21] I.I. Creaser, R.J. Geue, J.M. Harrowfield, A.J. Herlt, A.M. Sargeson, M.R. Snow, J. Springborg, J. Am. Chem. Soc. 104 (1982) 6016.
[22] A.G. Lappin, A. McAuley, Adv. Inorg. Chem. 32 (1988) 241.
[23] (a) M.P. Suh, S.-G. Kang, M.S. Lah, Inorg. Chem. 28 (1989) 1602;

(b) M.P. Suh, S.-G. Kang, V.L. Goedken, S.-H. Park, Inorg. Chem. 30 (1991) 365;
(c) S.-G. Kang, K. Ryu, M.P. Suh, J.H. Jeong, Inorg. Chem. 36 (1997) 2478.
[24] A. McAuley, D.G. Fortier, D.H. Macartney, T.W. Whitcombe, C. Xu. J. Chem. Soc. Dalton Trans. (1994) 2071.
[25] P.S. Pallavicini, A. Perotti, A. Poggi, B. Seghi, L. Fabbrizzi, J. Am. Chem. Soc. 109 (1987) 5139.
[26] K. Wieghardt, W. Walz, B. Nuber, J. Weiss, A. Ozarowski, H. Stratemeier, R. Reinen, Inorg. Chem. 25 (1986) 1650.
[27] I. Zilbermann, M. Winnik, D. Sagiv, A. Rotman, H. Cohen, D. Meyerstein, Inorg. Chim Acta. 240 (1995) 503.
[28] P.V. Bernhardt, L.A. Jones, P.C. Sharpe, J. Chem. Soc. Dalton Trans. (1997) 1169.
[29] T.J. Atkins, J.E. Richman, W.F. Oettle, Org. Synth. 58 (1978) 86.
[30] J.S. Bradshaw, K.E. Krakowiak, R.M. Izatt, J. Heterocycl. Chem. 26 (1989) 1431.
[31] S. Brandes, S. Lacour, F. Denat, P. Pullumbi, R. Guilard, J. Chem. Soc. Perkin Trans. 1 (1998) 639.
[32] A. Bencini, A. Bianchi, C. Bazzicalupi, M. Ciampolini, P. Dapporto, V. Fusi, M. Micheloni, N. Nardi, P. Paoli, B. Valtancoli, J. Chem. Soc. Perkin 2 (1993) 115.
[33] M. Ciampolini, M. Micheloni, F. Vizza, F. Zanobini, S. Chimichi, P. Dapporto, J. Chem. Soc. Dalton Trans. (1986) 505.
[34] A. Bencini, A. Bianchi, M. Ciampolini, S. Chimichi, P. Dapporto, M. Micheloni, P. Paoli, B. Valtancoli. J. Chem. Soc. Chem. Commun. (1990) 174.
[35] J. Springborg, P. Kofod, C.E. Olsen, H. Toftlund, I. Sotøfte, Acta Chem. Scand. 49 (1995) 547.
[36] L. Broge, I. Sotøfte, C.E. Olsen, J. Springborg, Inorg. Chem. 40 (2001) 3124, and references therein.
[37] A. Bencini, A. Bianchi, M. Ciampolini, E. Garcia-Espana, P. Dapporto, M. Micheloni, P. Paoli, J.A. Ramirez, B. Valtancoli. J. Chem. Soc. Chem. Commun. (1989) 701.
[38] A. Bencini, A. Bianchi, A. Borselli, M. Ciampolini, P. Dapporto, E. Garcia-Espana, M. Micheloni, P. Paoli, J.A. Ramirez, B. Valtancoli, Inorg. Chem. 28 (1989) 4279.
[39] R. Collison, N.W. Allcock, T.J. Hubjn, D.H. Busch, J. Coord. Chem. 52 (2001) 317.
[40] R. Kowallick, M. Neuburger, M. Zehnder, T.A. Kaden, Helv. Chim. Acta 80 (1997) 948.
[41] M. Rodopoulos, T. Rodopoulos, J.N. Bridson, L.-I. Elding, S.J. Rettig, A. McAuley, Inorg. Chem. 40 (2001) 2737.
[42] K.A. Beveridge, A. McAuley, C. Xu, Inorg. Chem. 30 (1991) 2074.
[43] F. Denat, S. Lacour, S. Brandes, R. Guilard, Tet. Lett. 38 (1997) 4417.
[44] S. Brandes, F.Denat, F. Rabiet, F. Barbette, P. Pullumbi, R. Guilard, Eur. J. Org. Chem. (1998) 2349.
[45] A.M. Ingham, Chao Xu, T.W.Whitcombe, Chengtian Xu, J.N.Bridson, A. McAuley, Canad. J. Chem. 80 (2002) in press.
[46] C. Bazzicalupi, A. Bencini, A. Bianchi, C. Giorgi, V. Fusi, A. Masotti, B. Valtncoli, A. Roque, F. Pina, J. Chem. Soc. Chem. Commum. (2000) 561.
[47] B. Alpha, E. Anklam, R. Deschenaux, J.-M. Lehn, M. Pietraszkiewicz, Helv. Chim. Acta 71 (1988) 1042.
[48] M. Cesario, J. Guilhem, C. Pascard, E. Anklam, R. Deschenaux, J.-M. Lehn, Helv. Chim. Acta 74 (1991) 1157.
[49] M.J. Hynes, B. Maubert, V. McKee, R.M. Town, J. Nelson, J. Chem. Soc. Dalton Trans. (2000) 2853.
[50] E.K. Barefield, D. Cheung, D.G. Vanderveer, J. Chem. Soc Chem. Commun. (1981) 302.
[51] I. Murase, S. Ueno, S. Kida, Inorg. Chim Acta 111 (1986) 57.
[52] R.W. Hay, G.A. Lawrance, N.F. Curtis, J. Chem. Soc. Perkin 1 (1975) 591.
[53] D.G. Fortier, A. McAuley, Inorg. Chem. 28 (1989) 655.
[54] D.G. Fortier, A. McAuley, J. Am. Chem. Soc. 112 (1990) 2640.
[55] E.K. Barefield, F. Wagner, K.D. Hodges, Inorg. Chem. 15 (1976) 1370.
[56] A.I. Ingham, T. Rodoupoulos, A. McAuley, unpublished results.
[57] C.Xu, A. McAuley, unpublished results.
[58] (a) B. Bosnich, C.K. Poon, M.L. Tobe, Inorg. Chem. 4 (1965) 1102;
(b) B. Bosnich, M.L. Tobe, G.A. Webb, Inorg. Chem. 4 (1965) 1109.
[59] S. Subramanian, A. McAuley, to be published.
[60] F. Rabiet, F. Denat, R. Guilard, Synth. Commun. 27 (1997) 979.
[61] A. Damsyik, P.J. Davies, C.I. Keeble, M.R. Taylor, K.P. Wainwright, J. Chem. Soc. Dalton Trans. (1998) 703.
[62] T.-H. Ahn, J. Kim, L.F. Lindoy, J. Wang, Aust. J. Chem. 52 (1999) 1139.
[63] J. Springborg, U. Pretzmann, C.E. Olsen, Acta Chem. Scand. 50 (1996) 294.
[64] K.R. Coulter, to be published.
[65] M. Micheloni, J. Coord. Chem. 18 (1988) 3.
[66] M. Micheloni, Comments Inorg. Chem. 8 (1988) 79.
[67] J. Springborg, C.E. Olsen, I. Søtofte, Acta Chem. Scand. 49 (1995) 555.
[68] C. Xu, A. McAuley, unpublished observations.
[69] T. Barclay, S. Subramanian, A. McAuley, J. Chem. Soc. Chem. Commun. (2002) 170.
[70] E.C. Constable, L.Y. Chung, J. Lewis, P. Raithby, J. Chem. Soc. Chem. Commun. (1986) 1719.
[71] G. Hafelinger, in: S. Patai (Ed.), The Chemistry of Amidines and Imidates, Interscience, New York, 1975, pp. 1–84.
[72] D.G. Fortier, unpublished observations.
[73] M.A. Donnelly, M. Zimmer, Inorg. Chem. 38 (1999) 1650.
[74] T.W. Hambley, J. Chem. Soc. Chem. Commun. (1984) 1228.
[75] L.Y. Martin, L.J. De Hayes, L.J. Zompa, D.H. Busch, J. Am. Chem. Soc. 96 (1974) 4046.
[76] G.J. McDougall, R.D. Hancock, J.C.A. Boeyens, J. Chem. Soc. Dalton Trans. (1978) 1438.
[77] K.R. Coulter, A. McAuley, S.J. Rettig, Canad. J. Chem. 79 (2001) 930.
[78] M. Rodopoulos, unpublished results.
[79] G. Hunter, A. McAuley, T.W. Whitcombe, Inorg. Chem. 27 (1988) 2634.
[80] T. Rodopoulos, unpublished observations.
[81] L. Broge, U. Pretzmann, N. Jensen, I. Søtofe, C.E. Olsen, J. Springborg, Inorg. Chem. 40 (2001) 2323.
[82] I. Bkouche-Waksman, J. Guilhem, C. Pascard, B. Alpha, R. Deschenaux, J.-M. Lehn, Helv. Chim. Acta 74 (1991) 1163.
[83] F.A. Cary, R.J. Sundberg (Eds.), Advanced Organic Chemistry, Part B, Plenum Press, New York/London, 1990, p. 467.
[84] L.J. Zompa, T.N. Margulis, Inorg. Chim. Acta 45 (1980) L263.
[85] S. Hart, J.C.A. Boeyens, J.P. Michael, R.D. Hancock, J. Chem. Soc. Dalton Trans. (1983) 1601.
[86] R.I. Haines, A. McAuley, Inorg. Chem. 19 (1980) 719.